Author Manuscript

Author Manuscript

Author Manuscript

Author Manuscript

HHS Public Access

Author manuscript

Brain Res. Author manuscript; available in PMC 2015 May 05.

Published in final edited form as:

Brain Res. 2008 November 6; 1239: 107–118. doi:10.1016/j.brainres.2008.08.043.

Membrane disruption: An early event of hair cell apoptosis induced by exposure to intense noise

Bo Hua Hu[1,*] and **Gui Liang Zheng**[1,2]

[1]Center for Hearing and Deafness, State University of New York at Buffalo, Buffalo, NY 14214, USA

[2]Institute of Otolaryngology, PLA General Hospital, Beijing, 100853, China

Abstract

Membrane leakage has been found in hair cells undergoing apoptosis following exposure to intense noise. However, it is not known whether this membrane damage is the consequence of apoptotic degeneration or direct mechanical stress. The current study was designed to investigate whether membrane damage occurred before the onset of apoptosis and to determine the level of the membrane damage. Chinchillas were exposed to an impulse noise at 155 dB peak SPL. The noise-induced membrane damage was assessed functionally, using membrane tracers with graded molecular sizes (propidium iodide and FITC-dextrans with molecular sizes of 3, 40, 500, and 2000 kDa), and morphologically, using DiO staining and semithin sections. The study revealed two major findings. First, exposure to intense noise caused a rapid increase in membrane permeability, and the onset of membrane leakage preceded the manifestation of nuclear condensation. This indicates that the early membrane damage observed in apoptosis is the direct consequence of mechanical stress. Second, the level of membrane damage was severe, allowing the entry of 3 kDa and 40 kDa FITC-dextrans, but the membrane was not completely broken down, as evidenced by the preservation of the ability to exclude 500 kDa and 2000 kDa FITC-dextrans molecules and the maintenance of the cell boundary. Notably, despite the membrane damage, hair cells continue to undergo the apoptotic process, leading to the generation of a type of apoptosis with early membrane damage.

Keywords

Plasma membrane; Permeability; Apoptosis; Hair cell; Acoustic trauma

© 2008 Elsevier B.V. All rights reserved.

*Corresponding author: Bo Hua Hu, Ph.D., Center for Hearing and Deafness, State University of New York, 137 Cary Hall, 3435 Main Street, Buffalo, NY 14214, USA, Phone: (716) 829-2001-(18), Fax: (716) 829-2980, bhu@acsu.buffalo.edu (BH Hu).

Presented in part in 37th Annual Meeting of Society of Neuroscience. San Diego, California, November, 2007

Publisher's Disclaimer: This is a PDF file of an unedited manuscript that has been accepted for publication. As a service to our customers we are providing this early version of the manuscript. The manuscript will undergo copyediting, typesetting, and review of the resulting proof before it is published in its final citable form. Please note that during the production process errors may be discovered which could affect the content, and all legal disclaimers that apply to the journal pertain.

Author Manuscript Author Manuscript Author Manuscript Author Manuscript

1. Introduction

Exposure to intense noise causes excessive motion of the basilar membrane of the cochlea, resulting in structural failure of the organ of Corti. At the tissue level, structural failure includes the split of the reticular lamina and the detachment of outer hair cells from the Deiters' cells (Hamernik et al., 1984; Henderson and Hamernik, 1986; Saunders et al., 1985). At the cellular level, structural damage manifests in a range of morphological defects, including plasma membrane leakage.

The plasma membrane is an essential component of a cell. It defines the cell boundary and maintains cell viability. Importantly, the plasma membrane is vulnerable to acoustic trauma. In this regard, several earlier studies have implicated membrane dysfunction in noise-induced cochlear pathogenesis. Mulroy et al. (Mulroy et al., 1998) showed a temporary increase of the plasma membrane permeability to Lucifer yellow, a molecular marker of membrane leakage, after exposure to a mild level of noise. Ahmad et al. (Ahmad et al., 2003) demonstrated trapped carbon spheres within the hair cells in cochlear lesions, indicative of the occurrence of membrane breakdown. Although these studies clearly link membrane breakdown to acoustic trauma, the role of membrane damage in hair cell death has not been established.

In the cochlea, sensory cells (both outer and inner hair cells) are the most vulnerable type of cells to acoustic trauma. Over the last few years, there have been intensive studies on the pathways of hair cell death following exposure to intense noise (Bohne et al., 2007; Hu et al., 2000; Nicotera et al., 2001; Niu et al., 2003; Shizuki et al., 2002; Van De Water et al., 2004; Wang et al., 2002; Yang et al., 2004; Ylikoski et al., 2002). These studies have documented multiple modes of cell death, with apoptosis being the primary cell death pathway responsible for the pathogenesis of cochlear lesions. Apoptosis has been found primarily in the early phase of cochlear pathogenesis (Hu et al., 2002; Yang et al., 2004). Acute apoptosis has two features. Temporally, it takes place prior to the generation of necrosis following exposure to noise, suggesting that apoptosis is the initial mode of cell death. Spatially, it takes place in the center of cochlear lesions, where hair cells receive the maximal level of mechanical stress. These temporal and spatial profiles of acute apoptosis suggest that this type of apoptosis is associated with direct mechanical stress.

Apoptosis exhibits a range of biological and morphologic changes, of which membrane leakage is one. The relationship between acute apoptosis and membrane leakage has been observed in noise-traumatized hair cells. Using propidium iodide (PI) as a membrane tracer, Hu (Hu, 2007) demonstrated that all hair cells displaying the signs of the later phase of nuclear morphology of apoptosis, such as nuclear fragmentation or marked nuclear condensation, show the signs of membrane leakage. Surprisingly, a hair cell can lose its membrane integrity when its nuclear condensation is mild and its mitochondrial membrane potential is still active (Hu, 2007).

The finding of early membrane damage appears to contradict the conventional view of apoptosis that posits that membrane integrity is preserved at the early stage (Lo et al., 1995; Majno and Joris, 1995). Indeed, the preservation of membrane integrity has been considered

Author Manuscript Author Manuscript Author Manuscript Author Manuscript

the hallmark of apoptosis. It prevents the early release of cellular contents during apoptosis, a key mechanism for preventing an inflammatory response in the host tissues. Loss of membrane integrity is a typical sign of necrosis. It occurs when a cell is subjected to a severe pathological insult or during the late phase of apoptosis, when apoptosis shifts to necrosis. Although the role of the plasma membrane in regulating cell death propensity toward apoptosis or necrosis has been well established, it is still not clear whether cells can die through the process of apoptosis when the plasma membrane is the initial target of a pathological insult.

Given that acoustic stimuli can directly traumatize the plasma membrane, we hypothesized that the membrane damage observed in the early stage of acute apoptosis is the initial event of apoptosis and is associated with direct mechanical stress. We further hypothesized that membrane damage does not involve a complete structural breakdown, as occurs in necrosis, so that the membrane-damaged cells can still enter the apoptotic pathway. To test the hypotheses, we developed a technique of *in vivo* cochlear staining. With this method, we investigated the temporal sequence of the occurrence of membrane damage and acute apoptosis, as well as examined the magnitude of membrane damage. Specifically, the following three questions were addressed: (1) Does membrane leakage take place prior to the onset of apoptosis? (2) Can hair cells having membrane leakage enter and remain in the apoptotic pathway? (3) What level of membrane damage do apoptotic cells have? The current study revealed a type of apoptosis, featuring early membrane damage in noise-traumatized hair cells.

2. Results

Although exposure to intense noise damaged various structures in the cochlea, injuring both hair cells and supporting cells in the organ of Corti, we focused on the description of the hair cell apoptosis in the current study, because hair cells are the primary target of acoustic trauma and the aim of the current study was to delineate the nature of hair cell apoptosis.

2.1. In vivo cochlear perfusion causes a mild loss of hearing sensitivity

ABR thresholds were measured to assess the influence of the cochlear perfusion on cochlear function. Fig. 1 compares the ABR thresholds before and after the cochlear perfusion. Note that both the membrane tracer-treated ears and the artificial perilymph-treated control ears display 5–15 dB threshold shifts across the five tested frequencies after the cochlear perfusion. However, the differences in these shifts are not statistically significant (two-way ANOVA, $p > .05$). This indicates that the cochlear perfusion had a minor influence on cochlear function. Because there was no difference between the two treatments, the membrane tracers themselves appeared to have no detectable toxic effect on cochlear function.

2.2. Normal outer hair cells exhibit a low level of uptake of FITC-Dx

We first examined the uptake of FITC-Dx in the normal organs of Corti. We found a weak, but consistent, FITC-Dx internalization of 3 kDa and 40 kDa FITC-Dx in outer hair cells. In contrast, when the cochleae were stained with 500 kDa or 2000 kDa FITC-Dx, there was no

Author Manuscript Author Manuscript Author Manuscript Author Manuscript

detectable fluorescence in the outer hair cells. The basic pattern of the FITC fluorescence was similar in the 3 kDa FITC-Dx -treated and 40 kDa FITC-Dx-treated ears.

Figs. 2A to 2D show typical patterns of the 40 kDa FITC-Dx staining, and Fig. 2G shows a 3 kDa FITC-Dx staining. Three features are clearly visible. First, the distribution of FITC-Dx fluorescence is cell-type specific. Only the outer hair cells display the fluorescence, whereas the inner hair cells and supporting cells lack the fluorescence. Second, not all the outer hair cells exhibited the FITC-Dx fluorescence. Figs. 2A to 2D show typical patterns of FITC-Dx staining in four sections of the organ of Corti. The location of these sections in the organ of Corti is presented in 2E. Note that there is no positive FITC-Dx cell in the basal extreme (2A). Beginning with the first turn, the FITC-Dx fluorescence starts to emerge in a small number of outer hair cells (Fig. 2B). The number of dextran-positive cells increases in the second turn (Fig. 2C). From the third cochlear turn, virtually all outer hair cells display the FITC-Dx fluorescence (Fig. 2D). The distribution pattern of FITC-Dx positive cells along the organ of Corti is presented in the cochleogram in Fig. 2F. The cochleogram shows that the number of outer hair cells showing the FITC-Dx fluorescence increases from the basal to the apical portion of the organ of Corti.

Although the distribution patterns of 3 kDa and 40 kDa FITC-Dx labeling was similar in the organ of Corti, their cellular distribution was different. In the 3 kD FITC-Dx-stained cells, the fluorescence appeared in both the cytosol and the nucleus (indicated by the arrows in 2G; see the inset for a high magnification view), whereas in the 40 kDa dextran-treated cells, the fluorescence appeared only in the cytosol, leaving the nuclear region void of fluorescence (the insert in 2B). The results suggest that 3 kDa dextran molecules are capable of passing through both the plasma membrane and the nuclear membrane, whereas the 40 kDa molecules pass through only the plasma membrane.

We then examined the permeability of the membrane to PI in the normal organs of Corti. The PI fluorescence was absent in both the PI-stained and PI- FITC-Dx-double stained organs of Corti (data not shown). The absence of the PI fluorescence suggests that all hair cells and supporting cells maintained their viability in the *in vivo* stained cochleae.

2.3. Occurrence of membrane leakage precedes the manifestation of nuclear condensation

The presence of apoptosis was identified using the nuclear morphology. The nature of apoptosis was further confirmed with the TUNEL assay and caspase-3 staining. Fig. 3A shows a typical TUNEL from a cochlea collected at 5 min after the noise exposure. Note that the outer hair cells showing nuclear condensation exhibit TUNEL fluorescence (indicated by the arrows; the yellow is due to the combination of the red PI fluorescence and the green TUNEL fluorescence). Fig. 3B shows a typical caspase-3 staining. Again, the outer hair cells showing nuclear condensation have strong caspase-3 activity (the green fluorescence indicated by the arrows). Because the nuclear morphology coordinated well with TUNEL or caspase-3 staining, we used the nuclear morphology as the indicator of apoptosis in the current study. Based on the nuclear morphology, the progression of hair cell degeneration observed at 5 min and 30 min after the noise exposure was divided into three stages.

Author Manuscript Author Manuscript Author Manuscript Author Manuscript

Stage I. Pre-nuclear condensation: Stage I pathology was observed in the cochleae collected at 5 min after the noise exposure. At this stage, there was no detectable nuclear condensation or nuclear swelling. However, membrane leakage was visible. Fig. 4A shows typical examples of membrane leakage. The text (1, 2, 3, and 4) in the figure point to four outer hair cell nuclei showing a gradient increase in the PI fluorescence (the insert presents a comparison of the gray levels of these four cells). Note that their shape and size remain unchanged and that their nucleoli are clearly visible. Adjacent outer hair cell nuclei lack the PI fluorescence and are barely visible. To inspect their nuclear morphology, we digitally enhanced the image, so that all the outer hair cell nuclei in this region became visible. Fig. 4B is the enhanced version of Fig. 4A. Note that three rows of outer hair cells appear disarranged, but the nuclei are in normal shape and size. At this stage, there is no detectable nuclear condensation or nuclear swelling.

Stage II. Appearance of nuclear condensation: Stage II pathology was also observed in the cochleae collected at 5 min after the noise exposure. At this stage, the hair cell pathology was characterized by the presence of nuclear condensation with the strong PI fluorescence. Fig. 5A shows examples of condensed nuclei. Note that the nuclei exhibit a bright PI fluorescence, an indication of membrane leakage (arrows). At this time point, no swollen nuclei were observed, implying that the initial cell death pathway in noise-induced hair cell pathogenesis is apoptotic.

To quantify the initial damage observed at 5 min after the noise exposure, we counted the number of FITC-Dx-stained outer hair cells and documented their distribution in the organ of Corti. Fig. 5B is a cochleogram showing the distribution and the number of PI-positive hair cells in the organ of Corti. The cochleogram shows that the positively-stained cells appeared in the cochlear regions around the upper second cochlear turn, which is according to our previous observation (Harris et al., 2005; Hu et al., 2006), the maximally-damaged cochlear section.

Stage III. Appearance of both apoptotic and necrotic nuclei: Stage III pathology appeared in the cochleae collected at 30 min after the noise exposure. At this time point, swollen nuclei appeared in the cochlear lesions (arrowheads in Fig. 5D). Apoptotic cells showed different extents of nuclear condensation, and very condensed nuclei were commonly seen (arrows in Fig. 5D). The number of apoptotic cells was significantly greater than that of necrotic cells, with a ratio of approximately 10 to 1. Fig. 5C shows the distribution of apoptotic and necrotic cells in the organ of Corti. Note that hair cell lesions expanded toward both the basal and apical ends of the organ of Corti.

Collectively, these observations suggest that membrane leakage is an early event of outer hair cell degeneration, preceding the commitment of the cells to apoptosis or necrosis.

2.4. The level of membrane damage

The level of membrane damage in the apoptotic cells was assessed using FITC-Dx with graded molecular sizes. Following the exposure to the impulse noise, hair cells exhibited an increase in permeability to FITC-Dx with the molecular weights of 3 kDa and 40 kDa. Similar to PI-positive cells, the FITC-positive cells were distributed around the second

Author Manuscript Author Manuscript Author Manuscript Author Manuscript

cochlear turn. Figs. 6A and 6B show typical images of 3 kDa, and Figs. 6C and 6D show images of 40 kDa FITC-Dx-stained hair cells (A and C: the combined images of FITC-Dx and PI, B and D: FITC-Dx only). Note that a strong FITC-Dx fluorescence was present in outer hair cells. These strongly labeled cells have a strong PI fluorescence in the nuclei (arrows in A; arrows and arrowheads in C). 3 kDa and 40 kDa FITC-Dx staining exhibit a similar pattern of fluorescence distribution in the cytosol, but differ in the nucleus in the early stage of cell death. The 3 kDa FITC-Dx fluorescence appears in both the cytosol and nuclei (arrows in B). In contrast, the 40 kDa FITC-Dx fluorescence appears only in the cytosol, not in the nuclei (arrows in D). As the cell death process progresses, the 40 kDa FITC-Dx fluorescence appears in the nuclear region (arrowheads in D), usually after the nuclei become condensed.

As described in the section on normal cochlear staining, the normal outer hair cells exhibit a low level of FITC-Dx fluorescence. In noise-traumatized cochleae, a low level of FITC-Dx fluorescence was also seen in certain outer hair cells (indicated by the arrowhead in A, as well as in B). These cells usually lacked the PI fluorescence in nuclei (indicated by the arrowhead in A).

When the cochleae were stained with 500 kDa and 2 MDa FITC-Dx, there was no detectable FITC fluorescence in the hair cells. Figs. 7A and 7B show examples of 500 kDa (A) and 2000 kDa (B) FITC-Dx staining. Note that PI positive cells are visible (arrows). However, these cells lack the FITC-Dx fluorescence.

To ensure that the large molecules of FITC-Dx could stain hair cells, should the membrane become permeabilized, we perforated the hair cell membrane with Triton X-100. The triton X-100 solution (0.05% in the artificial perilymph) was perfused into the cochlea 30 min before loading the 500 kDa FITC-Dx solution. Fig. 7C shows an example of 500 kD dextran staining following the Triton X-100 treatment. Note that all the cells display a strong dextran fluorescence. This observation indicates that large molecular dextrans can permeate the cells if the membrane integrity is compromised. Collectively, examination of the level of membrane damage in apoptotic cells indicates that the membrane damage is severe, allowing permeability of macromolecules with a molecular size as large as 40 kDa.

2.5. Membrane morphology in apoptotic cells

In addition to the functional assessment of the plasma membrane, we examined its morphological integrity using the techniques of membrane staining and semithin sections. Fig. 8A shows the DiO-stained membranes and the PI-stained nuclei from a cochlea examined at 5 min after the noise exposure. The arrow in 8A points to an outer hair cell having a condensed nucleus. Figs. 8B and 8C show the membrane condition at two sections of the outer hair cell, one at the level of the cell body (B) and the other at the level of the nucleus (C). Note that the membrane continuity appears to be intact in this apoptotic cell. Fig. 8D is a typical image of a semithin section of the organ of Corti from a noise-traumatized cochlea. The arrows point to three outer hair cells. These cells exhibit condensed nuclei, but the cell boundary is clearly visible. These observations indicate that the plasma membrane of apoptotic cells, although severely damaged, was not completely broken down and was able to hold the intracellular organelles in place.

Author Manuscript Author Manuscript Author Manuscript Author Manuscript

3. Discussion

The current study examined the integrity of the plasma membrane and its relationship to apoptosis through a series of functional and morphological parameters. There were four major findings. First, exposure to intense noise causes a rapid increase in membrane permeability, which precedes the manifestation of nuclear condensation. Second, the level of membrane damage is severe, allowing the entry of 3 kDa and 40 kDa FITC-Dx, but the membrane was not completely broken down, as evidenced by the maintenance of the cell boundary. Third, the hair cells with the membrane leakage can still die by the process of apoptosis. Finally, normal outer hair cells exhibit a low level of uptake of 3 kDa and 40 kDa FITC-Dx.

Membrane damage and apoptosis

Two aspects of membrane damage were assessed in the current study. The first was the temporal relationship between the membrane damage and apoptosis, and the second was the magnitude of membrane damage. To assess the temporal relationship, we used the nuclear morphology as an index of apoptosis progression because: (1) nuclear condensation or fragmentation is the hallmark of apoptosis (Majno and Joris, 1995); (2) the morphological change in nuclei is an early sign of apoptosis induced by acoustic trauma (Hu et al., 2006); and (3) the nuclear change occurs in a step-by-step fashion. We found that the increase in membrane permeability appeared in hair cells without detectable signs of nuclear condensation or swelling, suggesting that the onset of membrane leakage preceded the onset of nuclear condensation.

To assess the extent of the membrane lesions, we used graded sizes of FITC-Dx molecules. We found a strong FITC fluorescence in hair cells when 3 kDa or 40 kDa FITC-Dx tracer was applied. In contrast, when 500 kDa or 2000 kDa FITC-Dx tracer was used, no fluorescence was observed in the hair cells. The results clearly indicate that the maximal size of FITC-Dx molecule that can pass through the cell membrane is between 40 kDa and 500 kDa. Based on the molecular dimension of the dextrans measured in a previous study (Read and Bacic, 1996), we estimate that the size of membrane breaks is somewhere between 3–9 nm. This level of membrane damage allows leakage of macromolecules from cells, but still confines most cellular organelles within the cell. The estimation is consistent with the morphological finding that the cell boundary is clearly visible in apoptotic cells.

Under stress, a cell can die by apoptosis or necrosis. One of the commonly used parameters for separating apoptosis from necrosis is the functional status of the plasma membrane. Apoptosis is characterized by maintenance of the functional integrity of the plasma membrane, whereas necrosis features early loss of the membrane integrity. This pattern of damage has been seen in many pathological conditions. When the damage is mild, the cells die by apoptosis; when the damage is severe, the cells die by necrosis. In traumatic brain or spinal cord injury, the central lesion in the site of the direct mechanical hit is characterized by rapid cell death via necrosis, with early membrane damage. Around the central lesion, subsequent cell death gradually develops, and the subsequent cell death is apoptotic. Apparently, in brain and spinal cord injuries, necrosis is associated with a direct mechanical hit, whereas the apoptotic cell death is associated with secondary metabolic disturbance.

Author Manuscript Author Manuscript Author Manuscript Author Manuscript

In the current study, the damage factor is also a mechanical trauma. However, in contrast to traumatic brain or spinal cord injury, the noise-induced injury has different patterns of damage. The center of lesion, where the cells receive the maximal mechanical stress, is characterized by the generation of apoptosis. Perhaps the most striking difference is the early onset of membrane damage in apoptosis. Even with severe membrane damage, the hair cells can still die by apoptosis.

The biological mechanism responsible for the differences in the cell response to mechanical damage between the cochlear hair cells and cells in non-cochlear systems is not clear. In noise-damaged hair cells, the membrane damage can be caused by two distinctive, but intermingled, mechanisms: direct mechanical injury and membrane deterioration as the apoptotic process progresses. Mechanical membrane damage is induced by direct mechanical stresses, such as stretching, shearing, bending, and compression/decompression. This acute membrane damage takes place during the noise exposure and manifests immediately after the exposure. In contrast, the deteriorative change in the membrane is associated with the loss of the homeostasis of the cells in the late phases of apoptosis. Certainly, manifestation of the deteriorative change lags behind the direct mechanical trauma. In the current study, the occurrence of membrane damage was virtually instant. This rapidity suggests that the cause of the early membrane leakage is direct mechanical stress.

It is possible that the unique architecture of the organ of Corti and the nature of acoustic overstimulation create a condition that preferentially targets the plasma membrane of hair cells. However, other cellular components may be less vulnerable to the mechanical stress. Thus, hair cells with severe membrane damage can still undergo the apoptotic pathway. This speculation is supported by two pieces of evidence. First, mitochondrial membrane potential, an important indicator of mitochondrial energy production, was found to function in hair cell that had lost the plasma membrane integrity and had exhibited nuclear condensation following exposure to an intense noise (Hu, 2007). Second, as revealed in the current study, the level of nuclear membrane damage is less severe than that of the plasma membrane. Therefore, even with the membrane disruption, the apoptotic machinery still functions, due to the preservation of other essential cellular structures and functions.

The finding of apoptosis with early membrane disruption leads us to rethink the impact of membrane leakage on neighboring viable cells. Noise-induced apoptosis, due to the early leakage of cellular contents, may pose a greater influence on the surrounding surviving cells than does typical apoptosis with an intact membrane. A marked cell swelling commonly seen around apoptotic cells (unpublished observation) may be related to the impact of membrane leakage. A rapid expansion of cochlea lesions following exposure to intense noise (Hu et al., 2002; Yang et al., 2004) may also be a consequence of the membrane leakage. It is thus important, in future research, to investigate the impact of membrane leaks on cochlear pathogenesis.

Uptake FITC-Dx in the normal hair cells

An unexpected finding of the current study was the presence of FITC-Dx fluorescence in normal outer hair cells. Two reasons suggest that the internalization of the FITC-Dx fluorescence was not caused by inner ear disturbance due to the animal surgery and cochlear

Author Manuscript Author Manuscript Author Manuscript Author Manuscript

perfusion. First, after the surgery for cochlear perfusion, the cochlear function is largely preserved, as evidenced by the occurrence of only minor threshold shifts of ABR. If a significant number of outer hair cells had pathological membrane leakage, we would expect to see a marked reduction of hearing sensitivity. Second, although the FITC-Dx fluorescence is present in outer hair cells, these cells were still able to exclude PI. The exclusion of PI, a smaller-sized membrane tracer than is FITC-Dx, suggests the preservation of membrane function in the outer hair cells showing the FITC-Dx fluorescence. Taken together, these observations suggest that the uptake of dextrans in normal outer hair cells is not an indication of pathological membrane leakage.

The mechanism by which outer hair cells uptake FITC-Dx molecules is not clear. One possible route of passage is endocytosis. Studies have shown that hair cells demonstrate the capacity for endocytosis in both apical and basal ends of the cells (Griesinger et al., 2002; Griesinger et al., 2004; Meyer et al., 2001). Macromolecules, such as horseradish peroxidase, can be transported into hair cells by endocytosis (Leake and Snyder, 1987). It is possible that FITC-Dx entry can be attributed to endocytosis. However, it is not known why the current study showed FITC-Dx fluorescence only in outer hair cells, whereas a previous study showed that both inner and outer hair cells demonstrate rapid endocytosis (Griesinger et al., 2004). Regarding the preferential distribution of the FITC-Dx fluorescence in the outer hair cells at the apical portion of cochlea, it is not known whether this pattern of spatial distribution is specific to the permeability mark of FITC-Dx or represents a general pattern of endocytosis. To our knowledge, there is no report on the spatial difference in the endocytosis capacity of hair cells along the organ of Corti. Future studies are warranted to address this concern.

The presence of FITC-Dx in normal hair cells affects the observation of the FITC-Dx alteration in noise-damaged hair cells. However, the influence is limited because: (1) the normal cells showing the FITC-Dx fluorescence are located in the middle and apical turns, whereas the noise damage takes place in the middle and basal portion of the organ of Corti; (2) the fluorescence intensity associated with noise trauma is much stronger than that observed in the normal condition; and (3) the noise-induced increase in the FITC fluorescence is accompanied by an increase in the PI fluorescence in nuclei. To avoid ambiguity in distinguishing between the noise-induced and the normally-existing FITC-Dx fluorescence, we used PI staining as a complementary parameter. Only when the nuclei exhibited PI fluorescence was the FITC-Dx fluorescence considered to be a noise-induced change.

4. Materials and methods

4.1. Animals and noise exposure

Adult chinchillas (450–650 g) were used in the study. The care and use of the animals reported in this study were approved by the State University of New York at Buffalo Institutional Animal Care and Use Committee.

An impulse noise was used to induce hair cell death. An impulse noise features unique acoustic properties, including high intensity and short duration. The high stimulus intensity

Author Manuscript Author Manuscript Author Manuscript Author Manuscript

causes instant cell damage, whereas the short duration allows us to assess the onset of the initial damage that otherwise would be masked by prolonged noise exposure.

The impulse noise has been used in our previous studies (Hight et al., 2003; Hu et al., 2006). It consisted of a series of 75 pairs of impulses (1 second between each pair) generated by a D/A converter on a signal processing board (Loughborough TMS 32020). The signals were routed through an attenuator (HP 350 D), a filter (Krohn-Hite 3550R), and a power amplifier (NAD 2200) to a loudspeaker (JBL 2360). The loudspeaker was positioned 5 cm in front of the animal's head. The noise level was measured using a sound level meter (Larson and Davis 800B), a preamplifier (Larson and Davis model 825), and a condenser microphone (Larson and Davis, LDL 2559). The microphone was positioned at the level of the animal's head. The level of the impulse noise was 155 dB (peak sound pressure level). The duration of the exposure was 75 seconds.

4.2. Assessment of membrane permeability

Membrane tracers: Two types of membrane tracers with different molecular sizes were used. Propidium iodide (PI), a small molecule tracer, was used for the assessment of membrane permeability, as well as for the illustration of nuclear morphology. Fluorescein-labeled, lysine-fixable dextrans (anionic) (FITC-Dx) are large molecule tracers. Four sizes of FITC-Dx (3, 40, 500, and 2000 kDa) were used to assess the magnitude of the membrane damage.

All the membrane probes were purchased from Invitrogen, and the staining solutions were freshly prepared before application. For the PI staining, the stock solution (1mg/ml) was diluted with artificial perilymph (142 mM NaCl, 5.37 mM KCl, 1.47 mM MgCl2, 2 mM CaCl2, and 10 mM HEPES) to generate a working solution (5 μg/ml). For the FITC-Dx solution, FITC-Dx was dissolved in the artificial perilymph to generate a working solution (2 mg/ml for 3 kDa and 40 kDa FITC-Dx; 5 mg/ml for 500 kDa and 2,000 kDa FITC-Dx).

FITC-Dx staining procedure: FITC-Dx staining was performed *in vivo*. The *in vivo* staining allowed us to load the staining solution before the noise exposure, so that the membrane changes that occurred during and shortly after the noise exposure could be assessed. We developed a surgical procedure to load the staining solution into the cochleae. This procedure maximized the protection of the middle and inner ear function, so that subsequent acoustic stimuli could be transmitted to hair cells without significant attenuation. The animal was anesthetized with a mixture of ketamine (35 mg/kg) and acepromazine (0.5 mg/kg). One cochlea was exposed through a conventional posterior approach. A small opening (approximately 0.2 mm in diameter) was drilled in the bony shell over the scala tympani in the basal turn of the cochlea. Another small opening was drilled in the bony shell over the posterior semicircular canal. Approximately 10 μl of a FITC-Dx solution with one molecular size was slowly perfused into the cochlea through the opening in the scala tympani at the rate of 2 μl/min with a syringe pump (SP100i, World Precision Instruments). The excessive perilymph was allowed to efflux through the opening on the posterior semicircular canal. After the perfusion, the cochlear openings were sealed with a tissue adhesive (Vetbond Tissue Adhesive 3M, USA) and the bulla was closed with dental cement.

Author Manuscript Author Manuscript Author Manuscript Author Manuscript

Using the same procedure, the contralateral ear of the animal was perfused with another FITC-Dx solution with a different molecular size. Immediately after the probe loading, the animal was exposed to the impulse noise. At 20 min after the noise exposure, the cochlea was perfused with the PI solution, and the PI solution was allowed to remain in the cochlea for 10 min. After the staining, the animal was sacrificed and the cochlea was fixed with 10% buffered formalin.

To assess the FITC-Dx staining in normal hair cells and the influence of the cochlear perfusion on the cochlea function, a group of control animals without exposure to noise received the FITC-Dx perfusion or the artificial perilymph perfusion. ABR thresholds were tested before and 30 min after the cochlear perfusion.

PI Staining procedure: PI staining was performed in one of three conditions. The first condition was *in vivo* staining. The second condition was also an *in vivo* staining, but was conducted as a counterstaining for another biochemical assay (a FITC-Dx staining or a caspase-3 staining). The third condition was performed in fixed cochlear tissues. It was also used as a counterstaining method for a biochemical assay (a TUNEL assay or a membrane staining).

For the *in vivo* staining, the staining solution was perfused into the cochlea using the procedure that has been described above for the FITC-Dx staining. Five animals received the PI perfusion, then the noise exposure. Five minutes after the noise exposure, the animals were sacrificed and the cochleae were fixed with 10% buffered formalin. Another five animals received a reversed order of the treatments, that is, the noise exposure first and then the PI staining. The animals were sacrificed at 30 min after the noise exposure and the cochleae were fixed.

For the *in vivo* counterstaining, the cochleae were first stained with a FITC-Dx or a caspase-3 assay *in vivo* (see the following sections). Upon completion of the initial staining, the cochleae were perfused with the PI solution. The staining solution was allowed to remain in the cochleae for 10 min. Then, the animals were sacrificed and the cochleae were fixed.

For the fixed-tissue staining, the cochleae were collected at a defined time after the noise exposure. Then the cochleae were fixed and dissected. The organ of Corti was first stained using the TUNEL or a membrane assay, and then the organs of Corti were transferred to the PI staining solution and incubated for 10 min.

4.3. Assessment of membrane morphology

4.3.1. Plasma membrane staining—3,3′-dioctadecyloxacarbocyanine perchlorate (DiO, Invitrogen, Inc.) was used to stain the plasma membranes of the hair cells. DiO was dissolved in dimethylformamide to generate the staining solution (10 μM). The animals were sacrificed at 5 or 30 min after the noise exposure and the cochleae were fixed with 10% buffered formalin. Then, the cochleae were dissected in PBS and the organs of Corti removed. The organs of Corti were incubated in the DiO solution for 2 min, rinsed with PBS, and then doubly stained with PI.

Author Manuscript Author Manuscript Author Manuscript Author Manuscript

4.3.2. Semithin sections of the organ of Corti—Hair cell morphology was examined using semithin sections of the organ of Corti from four cochleae collected at 30 min after the noise exposure. The method for preparing the semithin sections of the organ of Corti has been presented in our previous publication (Hu, 2007). Briefly, the cochleae were fixed first with 2.5% glutaraldehyde in phosphate buffer (pH 7.3–7.4) for 4 hrs, then with 1% OsO4 in phosphate buffer for 1 hr. Segments (2–3 mm) of the basilar membrane around the second cochlear turns, where the maximal noise damage occurred, were collected and then embedded in Epoxy resin. Sections of the organ of Corti (2 μm in thickness) were obtained with a Reichert Supernova Ultramicrotome and then stained with 1% toluidine blue. The specimens were mounted on slides and observed with a Zeiss microscope with a 63× oil immersion objective. Images of the specimens were photographed with a digital camera (Nikon, Coolpix 995).

4.4. Identification of apoptosis

Apoptotic hair cells were identified using the morphological criteria of nuclei that have been previously introduced (Yang et al., 2004). Briefly, apoptotic cells were identified through the exhibition of nuclear condensation. Nuclear condensation was defined as shrinking nuclei with an increase in the PI fluorescence. A typical sign of nuclear condensation was loss of the nucleus' visibility due to the increase in the PI fluorescence. The nature of apoptosis was confirmed by the following two biological assays of apoptosis.

4.4.1. terminal transferase dUTP nick end labeling (TUNEL) assay—Nuclear DNA fragmentation was detected through a TUNEL assay kit (Invitrogen, Inc.), using a procedure that has been described in a previous publication (Nicotera et al., 2003). Briefly, 5 min or 30 min after the noise exposure, the animals were sacrificed and the cochleae were fixed. The organs of Corti were incubated in the freshly prepared DNA-labeling solution containing 10 μl of reaction buffer, 0.75 μl of TdT enzyme, 8.0 μL of BrdUTP, and 31.25 μL of dH_2O for 16 hrs at room temperature. The tissues were stained with Alexa Fluor 488 dye-labeled anti-BrdU antibody in the rinse buffer (5 μL of antibody plus 95 μL of rinse buffer) at room temperature for 1 hr. The TUNEL labeled tissues were doubly stained with PI.

4.4.2. Detection of caspase-3 activity—The activity of caspase-3 was detected using a caspase-3 kit for FAM-DEVD-FMK (Intergen Company, USA). The staining procedure has been described in our previous publication (Nicotera et al., 2003). Briefly, the animals were anesthetized with a mixture of ketamine (35 mg/kg) and acepromazine (0.5mg/kg) 5 min after the noise exposure. The cochleae were surgically exposed and perfused with approximately 30 μl of the freshly prepared staining solution. The solution remained in the cochleae for 50 min. Then the cochleae were perfused with the PI solution. Ten minutes later, the cochleae were perfused with a manufacturer-provided buffer, followed by a manufacturer-provided fixative. The animals were sacrificed and the cochleae harvested.

4.5. Measurements of auditory brain stem responses (ABR)

ABR testing was conducted to determine the influence of probe loading on hearing thresholds in 8 control animals receiving the surgery of cochlear perfusion for probe loading without subsequent noise exposure. The testing was conducted before and 30 min after the

Author Manuscript Author Manuscript Author Manuscript Author Manuscript

cochlear perfusion. ABRs were elicited with tone bursts generated digitally (TDT, SigGen) and played out through a D/A converter (TDT, RP2.1, 100 kHz sampling rate) in the signal averaging system. Tone bursts were presented at 1, 2, 4, 8, and 16 kHz (0.5 ms rise/fall Blackman ramp, 1 ms duration, alternating phase) at the rate of 21 per second. The stimulus levels varied by 5 dB descending steps.

The ABR responses were recorded by three stainless steel needle electrodes placed subdermally over the vertex (positive) and the right and left mastoids (negative and ground electrodes) of the animal. The output of the electrodes was led to the head stage of a differential amplifier (TDT, RA4LI), followed by an amplifier (TDT, RA16PA), and then routed by a fiber optic cable to a real-time processor (TDT, RA16BA, 24 kHz sampling rate) that is part of an auditory evoked response averaging system controlled by TDT software (BioSig). The input signals were amplified (~50,000×), filtered (100–3000 Hz), processed with an artifact reject at 80% of the full scale, averaged (600 sweeps), and then stored and displayed on a computer. The ABR thresholds were defined as the lowest intensity that elicited a response.

4.6. Experimental procedures

At a defined time after the noise exposure, the animals were sacrificed. The cochleae were collected and fixed with 10% buffered formalin. The cochlea was dissected in 10 mM phosphate buffered saline to remove the bony shell, the lateral wall, the vestibular membrane and the tectorial membrane. The organ of Corti was separated from the modiolus and collected. After the dissection, the whole organ of Corti was either mounted on a slide for microscopic observation or further processed for a specific staining (DiO staining or TUNEL).

For the *in vivo* assessment of membrane permeability, the animals were treated by one of the following sequences: *in vivo* probe loading, then noise exposure, or vice versa. For other assays, the animals were first exposed to noise and then the cochleae were processed for a specified staining. Table 1 shows the number of cochleae used for each assay. For most assays, two cochleae from each animal were stained with different probes. Specifically, for the FITC-Dx staining, the two cochleae from each animal were treated with different sizes of FITC-Dx probes. For the other stainings, one cochlea was stained with PI in vivo and the other with DiO, or one ear with TUNEL and the other used for semithin sectioning. For caspase-3 staining, only one cochlea from each animal was used.

There were two types of control. The noise control, or the cochleae that did not receive the noise exposure, was used as a negative control. The perfusion control, or the cochlea perfused with only the artificial perilymph, was used to assess the potential influence of permeability markers on cochlear function.

4.7. Data analyses

All specimens were thoroughly examined with a fluorescence/biological microscope to identify cochlear lesions. The specimens were further examined using a confocal microscope (Zeiss LSM 510 META). The ability of confocal microscopy to scan a series of

Author Manuscript Author Manuscript Author Manuscript Author Manuscript

optical sections enabled us to obtain sequential images along the depth of the specimen. Because each type of cell in the organ of Corti, such as outer hair cells, Deiters' cells, and Hensen's cells, has a unique position in the 3-dimentional structure of the organ of Corti, these cells can be clearly identified and illustrated, without ambiguity. A series of confocal scanning photographs was taken from the sections of interest in the organ of Corti. The collected images were viewed with a manufacturer-provided software (LSM Image Examiner), which allowed us to observe cells positioned in any specified optical sections and to generate images showing a specified type of cell. We also used an image processing software (Image-Pro Plus 6.1) to enhance the weak fluorescence and to conduct a gray level analysis for Fig. 4A. For the image enhancement, the range of the gray level of the image was narrowed from 0–255 to 0–80, so that the weak fluorescence became visible. For the gray level analysis, the marked nuclei were individually selected, and the average gray level of each nucleus was calculated by the software.

Acknowledgments

This project was supported by the Grant NIDCD 5R03DC006181-03 and the New Faculty Start-up Funds from the College of Arts and Sciences, State University of New York at Buffalo.

Abbreviations

PI	propidium iodide
FITC-Dx	Fluorescein-labeled dextrans
TUNEL	terminal transferase dUTP nick end labeling

References

Ahmad M, Bohne BA, Harding GW. An in vivo tracer study of noise-induced damage to the reticular lamina. Hear Res. 2003; 175:82–100. [PubMed: 12527128]

Bohne BA, Harding GW, Lee SC. Death pathways in noise-damaged outer hair cells. Hear Res. 2007; 223:61–70. [PubMed: 17141990]

Griesinger CB, Richards CD, Ashmore JF. Fm1–43 reveals membrane recycling in adult inner hair cells of the mammalian cochlea. J Neurosci. 2002; 22:3939–52. [PubMed: 12019313]

Griesinger CB, Richards CD, Ashmore JF. Apical endocytosis in outer hair cells of the mammalian cochlea. Eur J Neurosci. 2004; 20:41–50. [PubMed: 15245477]

Hamernik RP, Turrentine G, Roberto M, Salvi R, Henderson D. Anatomical correlates of impulse noise-induced mechanical damage in the cochlea. Hear Res. 1984; 13:229–47. [PubMed: 6735931]

Harris KC, Hu B, Hangauer D, Henderson D. Prevention of noise-induced hearing loss with Src-PTK inhibitors. Hear Res. 2005; 208:14–25. [PubMed: 15950415]

Henderson D, Hamernik RP. Impulse noise: critical review. J Acoust Soc Am. 1986; 80:569–84. [PubMed: 3745686]

Hight NG, McFadden SL, Henderson D, Burkard RF, Nicotera T. Noise-induced hearing loss in chinchillas pre-treated with glutathione monoethylester and R-PIA. Hear Res. 2003; 179:21–32. [PubMed: 12742235]

Hu BH, Guo W, Wang PY, Henderson D, Jiang SC. Intense noise-induced apoptosis in hair cells of guinea pig cochleae. Acta Otolaryngol. 2000; 120:19–24. [PubMed: 10779180]

Hu BH, Henderson D, Nicotera TM. Involvement of apoptosis in progression of cochlear lesion following exposure to intense noise. Hear Res. 2002; 166:62–71. [PubMed: 12062759]

Author Manuscript Author Manuscript Author Manuscript Author Manuscript

Hu BH, Henderson D, Nicotera TM. Extremely rapid induction of outer hair cell apoptosis in the chinchilla cochlea following exposure to impulse noise. Hear Res. 2006; 211:16–25. [PubMed: 16219436]

Hu BH. Delayed mitochondrial dysfunction in apoptotic hair cells in chinchilla cochleae following exposure to impulse noise. Apoptosis. 2007; 12:1025–36. [PubMed: 17268771]

Leake PA, Snyder RL. Uptake of horseradish peroxidase from perilymph by cochlear hair cells. Hear Res. 1987; 25:153–71. [PubMed: 3104269]

Lo AC, Houenou LJ, Oppenheim RW. Apoptosis in the nervous system: morphological features, methods, pathology, and prevention. Arch Histol Cytol. 1995; 58:139–49. [PubMed: 7576866]

Majno G, Joris I. Apoptosis, oncosis, and necrosis. An overview of cell death. Am J Pathol. 1995; 146:3–15. [PubMed: 7856735]

Meyer J, Mack AF, Gummer AW. Pronounced infracuticular endocytosis in mammalian outer hair cells. Hear Res. 2001; 161:10–22. [PubMed: 11744276]

Mulroy MJ, Henry WR, McNeil PL. Noise-induced transient microlesions in the cell membranes of auditory hair cells. Hear Res. 1998; 115:93–100. [PubMed: 9472738]

Nicotera, T.; Henderson, D.; Hu, BH.; Zheng, XY. Noise exposure and mechanisms of hair cell death. In: Henderson, D.; Prasher, D.; Kopke, R.; Salvi, R.; Hamernik, R., editors. Noise Induced Hearing Loss: Basic Mechanisms, Prevention and Control. Noise Research Network Publications; London: 2001. p. 99-117.

Nicotera TM, Hu BH, Henderson D. The caspase pathway in noise-induced apoptosis of the chinchilla cochlea. J Assoc Res Otolaryngol. 2003; 4:466–77. [PubMed: 14534835]

Niu X, Shao R, Canlon B. Suppression of apoptosis occurs in the cochlea by sound conditioning. Neuroreport. 2003; 14:1025–9. [PubMed: 12802196]

Read, S.; Bacic, A. Plant Cell Wall Analysis. In: Linskens, HF.; Jackson, JF., editors. Modern Methods of Plant Analysis. Springer Verlag; Berlin: 1996. p. 63-80.

Saunders JC, Dear SP, Schneider ME. The anatomical consequences of acoustic injury: A review and tutorial. J Acoust Soc Am. 1985; 78:833–60. [PubMed: 4040933]

Shizuki K, Ogawa K, Matsunobu T, Kanzaki J, Ogita K. Expression of c-Fos after noise-induced temporary threshold shift in the guinea pig cochlea. Neurosci Lett. 2002; 320:73–6. [PubMed: 11849767]

Van De Water TR, Lallemend F, Eshraghi AA, Ahsan S, He J, Guzman J, Polak M, Malgrange B, Lefebvre PP, Staecker H, Balkany TJ. Caspases, the enemy within, and their role in oxidative stress-induced apoptosis of inner ear sensory cells. Otol Neurotol. 2004; 25:627–32. [PubMed: 15241246]

Wang J, Dib M, Lenoir M, Vago P, Eybalin M, Hameg A, Pujol R, Puel J. Riluzole rescues cochlear sensory cells from acoustic trauma in the guinea-pig. Neuroscience. 2002; 111:635–648. [PubMed: 12031350]

Yang WP, Henderson D, Hu BH, Nicotera TM. Quantitative analysis of apoptotic and necrotic outer hair cells after exposure to different levels of continuous noise. Hear Res. 2004; 196:69–76. [PubMed: 15464303]

Ylikoski J, Xing-Qun L, Virkkala J, Pirvola U. Blockade of c-Jun N-terminal kinase pathway attenuates gentamicin-induced cochlear and vestibular hair cell death. Hear Res. 2002; 166:33–43. [PubMed: 12062756]

Author Manuscript Author Manuscript Author Manuscript Author Manuscript

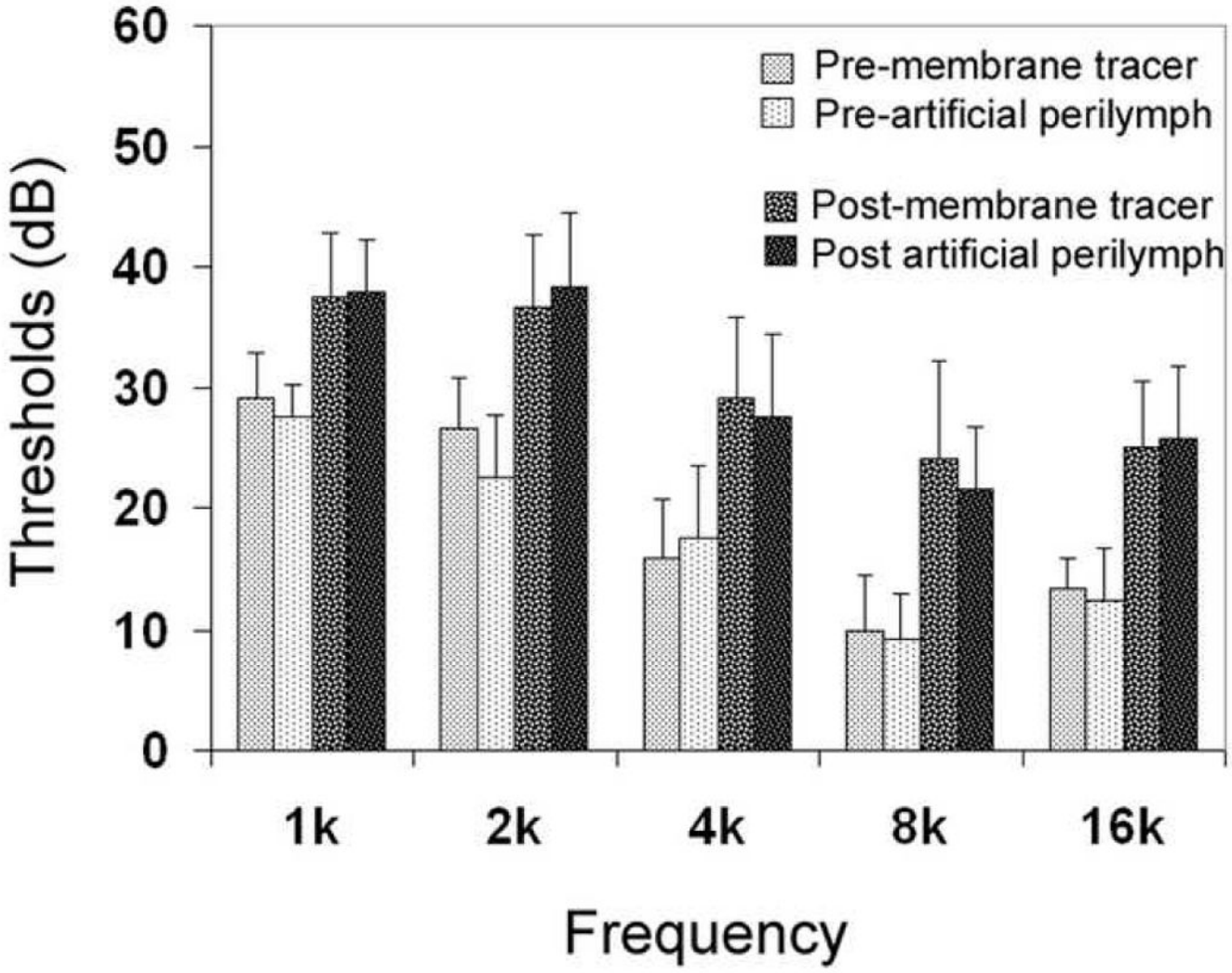

Figure 1.

Comparison of ABR thresholds among four experimental conditions. Note that both the membrane tracer-treated and the artificial perilymph-treated cochleae exhibit mild threshold shifts (8.3–16 dB) after cochlear perfusion. However, there was no statistically significant difference between them.

Author Manuscript Author Manuscript Author Manuscript Author Manuscript

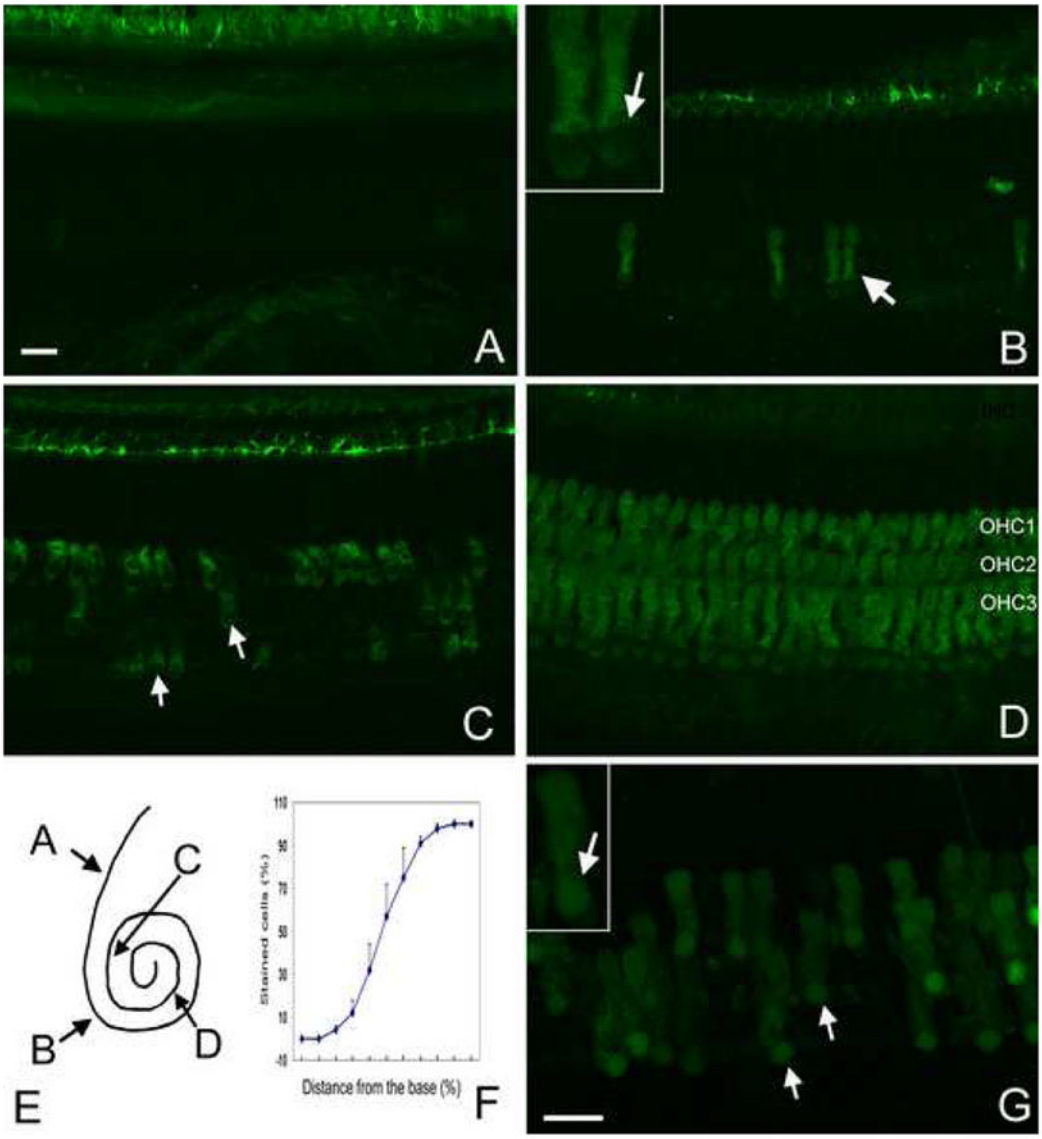

Figure 2.

FITC-Dx staining in normal cochleae. A to D: 40 kDa FITC-Dx staining in four regions of the organ of Corti: the base (A), the first turn (B), the second turn (C), and the third turn (D). E: The corresponding sites of these four regions in the organ of Corti. The insert in B shows the presence of the 40 kDa FITC dextran fluorescence in the cytosol, not the nuclei. F: The cochleogram showing the distribution of the FITC-Dx-stained outer hair cells along the organ of Corti. Note that from the base (left) to the apex (right) of the organ of Corti, the percentage of the positively stained cells increases. G: 3 kD FITC-Dx staining in the second turn of a normal cochlea. The insert shows that the fluorescence of 3 kDa FITC-Dx is presented in both the cytosol and the nuclei. Bar: 15μl.

Author Manuscript Author Manuscript Author Manuscript Author Manuscript

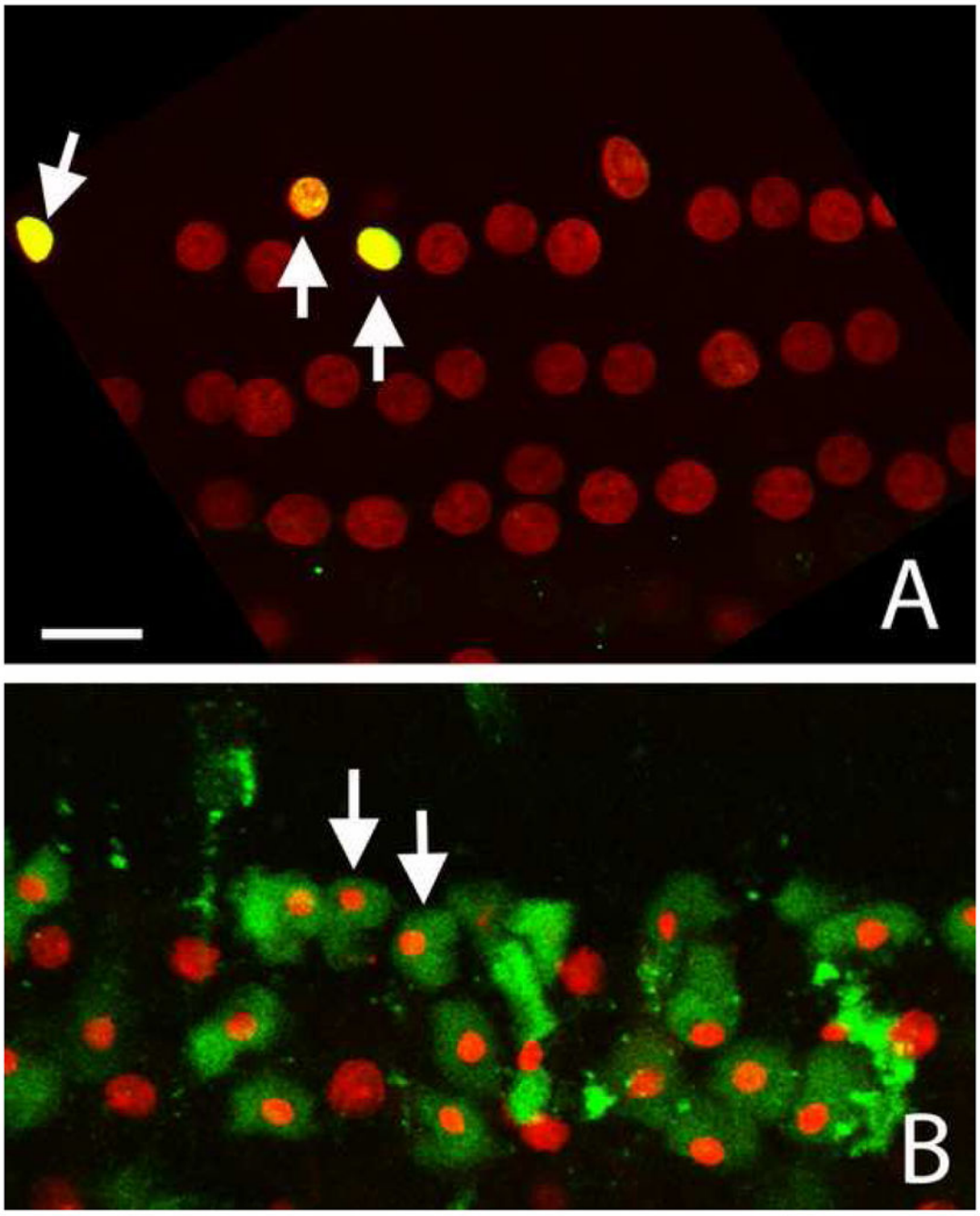

Figure 3.

Apoptotic cells showing positive TUNEL and caspase-3 staining. A: A typical TUNEL image. The condensed nuclei exhibit a strong TUNEL fluorescence (indicated by arrows). B: A typical caspase-3 staining. The cells showing nuclear condensation exhibit a strong caspase-3 fluorescence (green) in the cytosol (arrows). Both images show hair cells in the second cochlear turn. Bar: 12 μl.

Author Manuscript Author Manuscript Author Manuscript Author Manuscript

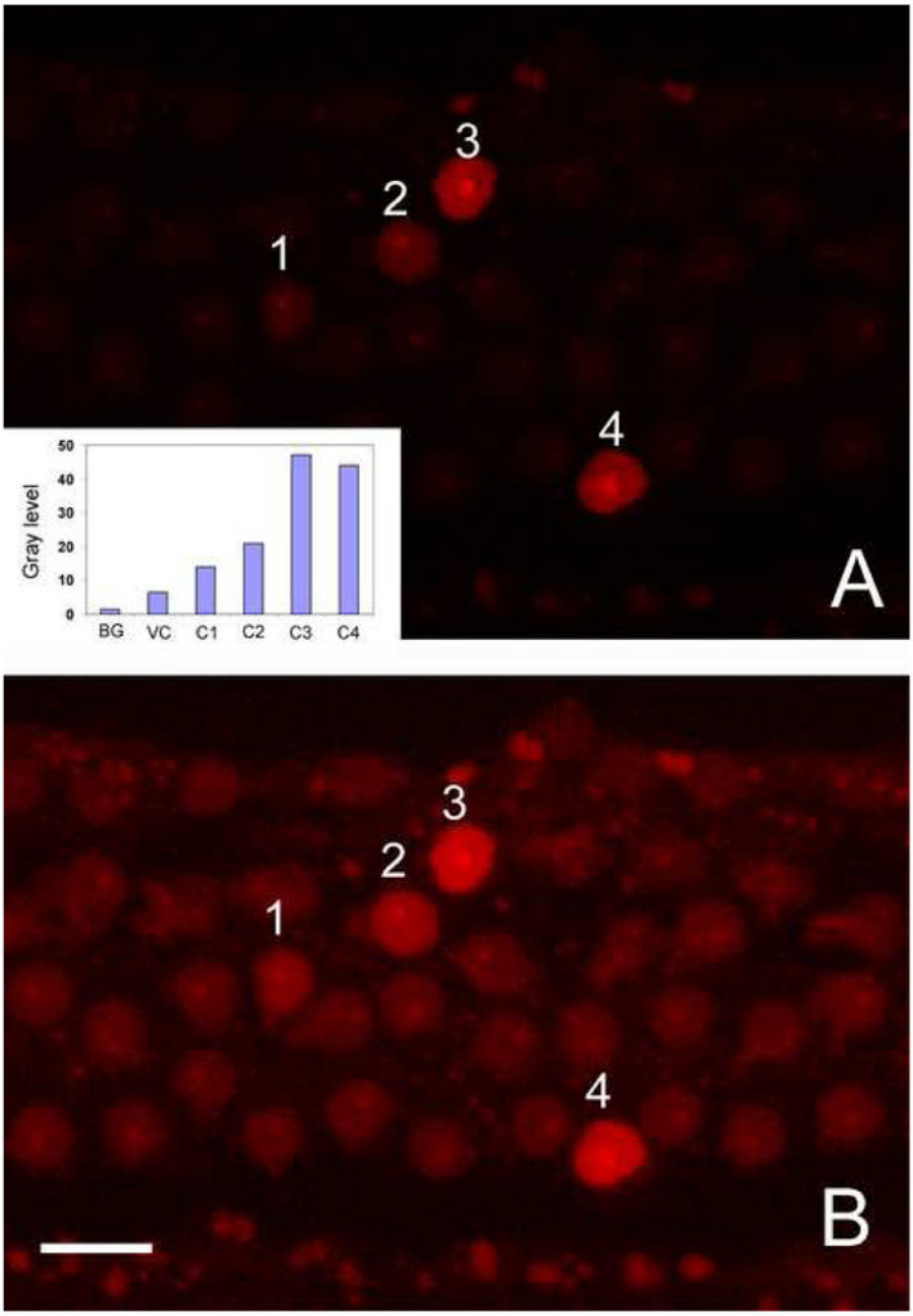

Figure 4.

Early membrane leakage in hair cells. A: PI staining shows the increase in plasma membrane permeability in hair cells of the second cochlear turn following exposure to the impulse noise. 1, 2, 3, and 4 in A indicate four nuclei showing different intensities of the PI fluorescence. The comparison of the gray levels of these cells, as well as the background (BG) and surrounding viable cells (VC), is present in the insert. Note that these PI-positive nuclei have a relatively normal size and texture. B: Digitally-enhanced image. The nuclei that are barely visible in 4A become visible after image processing. Note that all cells

exhibit the normal nuclear morphology. BG, VC, C1, C2, C3, and C4 in the insert represent the background, the viable cell, cell 1, cell 2, cell 3, and cell 4, respectively. Bar: 10μl.

Author Manuscript Author Manuscript Author Manuscript Author Manuscript

Author Manuscript Author Manuscript Author Manuscript Author Manuscript

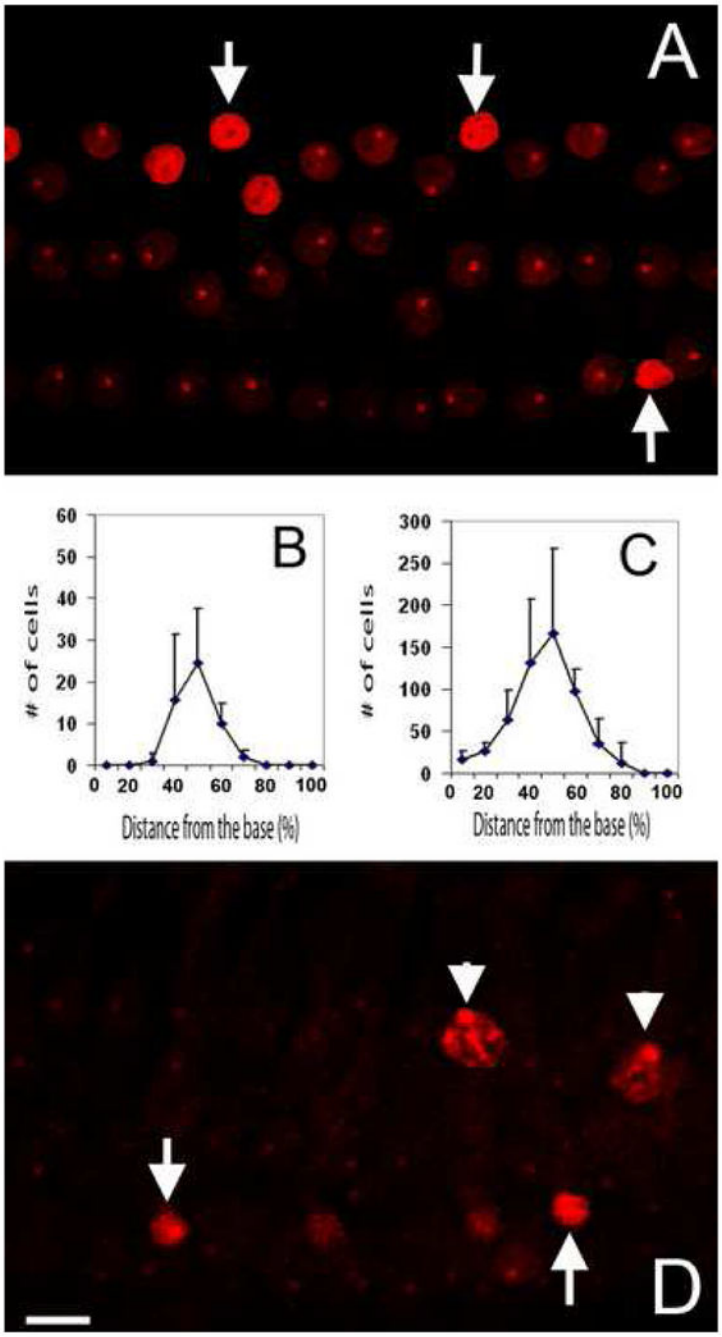

Figure 5.

Appearance of apoptosis and necrosis. A: A typical image showing the PI staining in an organ of Corti collected at 5 min after the noise exposure. Arrows indicate the condensed nuclei. B and C: The average distributions of the PI-stained cells in the organs of Corti processed at 5 min (B) or 30 min (C) after the noise exposure. D: Image showing PI staining in an organ of Corti processed at 30 min after the noise exposure. Arrows indicate the condensed nuclei. Arrowheads indicate swollen nuclei. Both images A and D show hair cells in the second cochlear turn. Bar: 10 μl.

Author Manuscript Author Manuscript Author Manuscript Author Manuscript

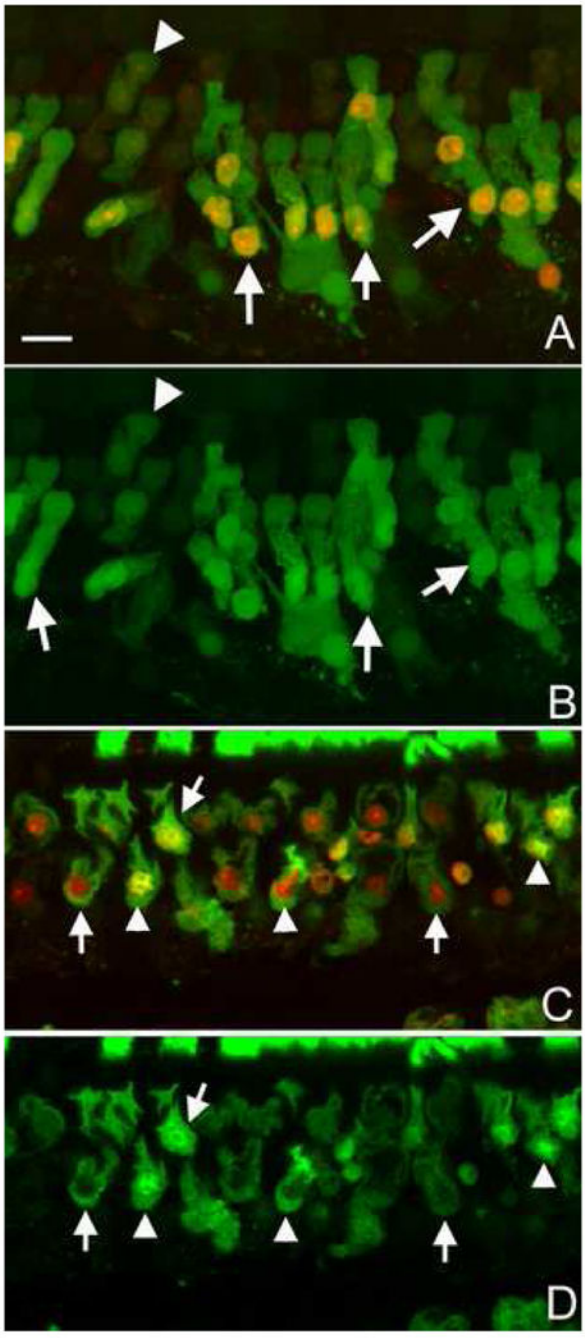

Figure 6.

Membrane leakage assessed by FITC-Dx labeling following exposure to the noise. A and B: Images of the 3 kDa FITC-Dx fluorescence (green) with the PI fluorescence (A) or without the PI fluorescence (B). Arrows indicate PI-stained cells. These cells also exhibit a strong FITC-Dx fluorescence. The arrowhead indicates a hair cell lacking the PI fluorescence. This cell has a weak FITC-Dx fluorescence. The FITC-Dx presents in both the cytosol and the nuclei. C and D: Images of the 40 kDa FITC-Dx fluorescence with the PI fluorescence (C) or without the PI fluorescence (D). Arrows indicate hair cells showing a strong FITC-Dx

Author Manuscript Author Manuscript Author Manuscript Author Manuscript

fluorescence in the cytosol. Arrowheads indicate the hair cells showing the FITC-Dx fluorescence in both the cytosol and nuclei. All the images show hair cells in the second cochlear turn. Bar: 20 μl.

Author Manuscript Author Manuscript Author Manuscript Author Manuscript

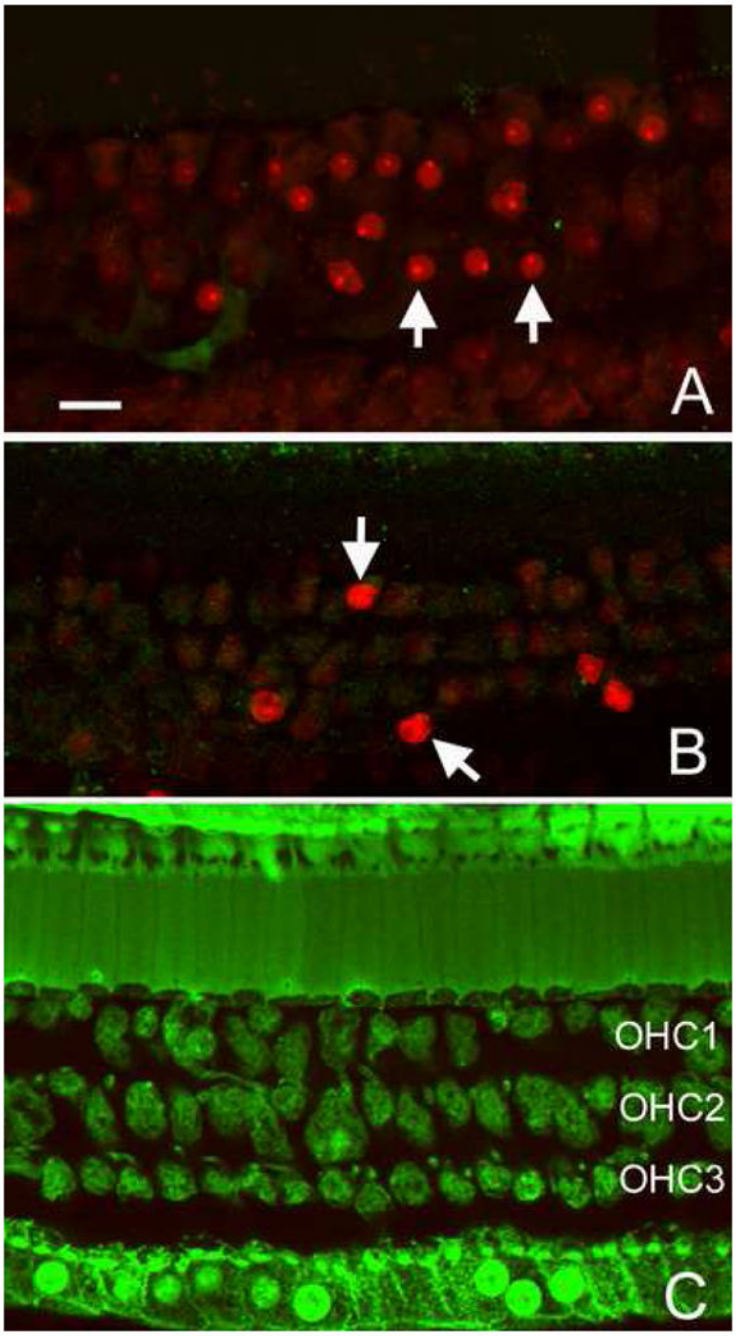

Figure 7.

Absence of the fluorescence of FITC-Dx with large molecular sizes following the noise exposure. A: A typical image of a 500 kDa FITC-Dx and PI-doubly-stained organ of Corti. B: An image of a 2000 kDa FITC-Dx and PI-doubly-stained organ of Corti. Arrows indicate outer hair cells exhibiting a strong PI fluorescence in the nuclei. These cells lack the FITC-Dx fluorescence. C: 500 kDa FITC staining in an organ of Corti treated with the Triton X-100 solution. Note that all the hair cells and supporting cells show a strong FITC-Dx

Author Manuscript Author Manuscript Author Manuscript Author Manuscript

fluorescence. Bar: 15μl. OHC1, OHC2, and OHC3 indicate the first, second, and third rows of outer hair cells, respectively. The images show hair cells in the second cochlear turn.

Author Manuscript Author Manuscript Author Manuscript Author Manuscript

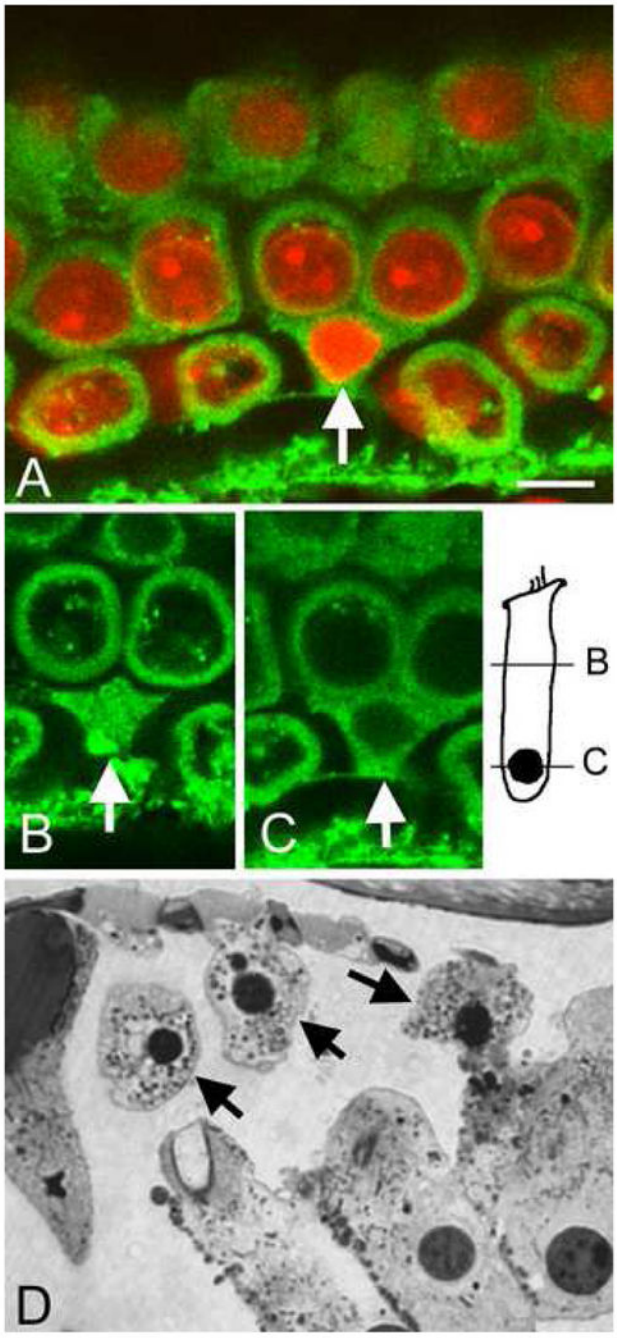

Figure 8.

Images showing the boundaries of apoptotic cells. A: A doubly-stained membrane (green fluorescence) and the nuclei (red fluorescence) from a cochlea stained at 5 min after the noise exposure. The arrow indicates a hair cell having the condensed nucleus. B and C: Typical examples of the membrane condition at two sites of the apoptotic cell: the cell body (B) and the nucleus (C). There is no detectable membrane break in the apoptotic cell. D: A typical image of a semithin section showing the side view of the hair cells. The arrows

indicate outer hair cells exhibiting condensed nuclei. These cells have a clear cell boundary. Bar: 5 μl. The images show hair cells in the second cochlear turn.

Author Manuscript Author Manuscript Author Manuscript Author Manuscript

Author Manuscript Author Manuscript Author Manuscript Author Manuscript

Table 1

Number of cochleae used for each assay

	5 min	30 min	Noise Control	Perfusion Control
FITC-Dx 3 kDa		6	4	4
FITC-Dx 40 kDa		6	4	4
FITC-Dx 500 kDa		6	4	4
FITC-Dx 2000 kDa		6	4	4
PI staining	5	5	3	3
DiO staining	5	5	3	
TUNEL assay	3	3	3	
Semithin section		4	2	
Caspase-3 staining		4	4	

Brain Res. Author manuscript; available in PMC 2015 May 05.